BOUNDARY LAYER-TRIPPING STUDIES ON CHARACTERISTICS OF NEAR-WAKE BEHIND A CAMBERED AIRFOIL

H.A. Abdalla

*Department of Mechanical Power Engineering,
Faculty of Engineering, Minufiya University,
Shebin El-Kom, Egypt*

ABSTRACT

This paper presents an experimental study to the effects of boundary layer-tripping on the aerodynamic performance and the near-wake which generates immediately behind the trailing edge of NACA-2415 airfoil sections. The airfoil was tripped by separately placing two different trip wires near the leading edge as an artificial roughness to induce rapid transition. The tripped and untripped airfoil were tested at different angles of attack to indicate the effects of pressure gradient and streamline curvature on its aerodynamic performance and the wake development behind the airfoil sections. Measurements included lift and drag coefficients, static pressure distributions, and mean velocity profiles in the wake region at Reynolds numbers between 3.5×10^4 and 1.92×10^5. The results of this experimental investigation showed that the aerodynamic performance of the airfoil is sensitive to the tripping mechanism. The drag coefficient of the airfoil increases due to the distorted velocity profiles in the wake region caused by the boundary layer tripping. The boundary layer tripping did not affect strongly the wake velocity profiles in the case of negative angles of attack and the wake velocity distributions are symmetric. Asymmetric velocity profiles are observed in the wake region as the angle of attack increases, for both tripped and untripped airfoils. The results indicated also that, the pressure gradient and the separation location on airfoil surfaces significantly control the growth of the wake. The effect of the boundary layer tripping on the growth of the wake width, the decay of the maximum velocity defect and similarity of wake profiles are discussed.

Keywords : Cambered airfoil, Boundary layer tripping, Wake properties, Aerodynamic.

1- INTRODUCTION

There are many engineering applications where turbulent boundary layer over curved surfaces are encountered, e. g. turbomachine blades, wings or airfoils and hubs of propellers. Boundary layer separation is usually due to a sufficiently strong adverse pressure gradient. Such adverse pressure gradient may caused by streamline curvature. At the rear of the airfoils where separation is most likely to occur, the free shear layers which are formed pass on downstream to form the wake of the airfoil. The flow separation and the subsequent wake greatly influence the drag and stability of the airfoils. The structure of the wake under the influence of streamline curvature is different form that of the wake without this effect. The effects of streamline curvature in a turbulent flow were recognized by many experimental investigations, e. g. So and Mellor [1, 2], Ramaprian and Shiraprasad [3], Bradshaw [4] and Castro and Bradshaw [5]. Their experimental results have shown that the turbulence structure, as well as the mean velocity profile, is changed considerably due to the effects of streamline curvature. Consequently, the wake development under such flow conditions is subjected to pressure gradient and curvature effects. The curvature and pressure gradient will significantly affect the mean velocity profiles and turbulent properties of the wake. The behaviour of the wakes in the presence of free-stream turbulence was studied in Refs. [6-8]. It was concluded that free-stream turbulence enhances wake mixing, growth rates, turbulence intensities and Reynolds stresses. The effects of pressure gradient and curvature on wake defect were investigated by Nakayama [9]. He carried out a systematic study of the effect of mild pressure gradient and mild streamline curvature on a small defect wake. The wake was subjected to mild curvature and mild pressure gradient by deflecting it by a thin plate at small angles of incidence in the external flow. The measured data indicate a strong sensitivity of turbulence quantities to the curvature and pressure gradient. In Ref. [10], an experimental investigation was conducted to characterized the development of asymmetrical turbulent wake generated by a rotating cylinder. With respect to the stationary cylinder, the velocity profiles are symmetrical around the position of the cylinder central plane. As the speed of cylinder rotation increases, these profiles become increasingly asymmetrical, especially in the near-wake region. The positions of the near-wake flow, where the maximum of the mean velocity defect occur, are laterally displaced in a direction consistent with the cylinder center. For peripheral velocity of the cylinder less than the free-stream velocity, the characteristic velocity and length scales for the mean flow are effectively equal to those of the stationary cylinder wake, because the shedding of Kármán vortices remains unaffected by rotation. As the peripheral velocity increases beyond that of the oncoming free-stream, however, the formation of Kármán vortices is inhibited and the values of the mean velocity defect, wake width, and intensities of the fluctuating velocity components are decreased.

In the range of Reynolds numbers of 10^4 to 10^6, Ref. [11], many complicated phenomena take place within the boundary layer, separation,

116

transition and reattachment could all occur within a short distance and affect the performance of the airfoil. At low Reynolds number, this separation may be occured over the entire rear of the airfoil and hence extended into the wake. However, in the low Reynolds number range, the boundary layer at the onset of the pressure rise may still be laminar, and thus unable to withstand any significant adverse pressure gradients. The performance of low Reynolds number airfoils is entirely dictated by the relatively poor separation resistance of the laminar boundary layer. Therefore, transition to turbulent flow must be accelerated for enhancing the airfoil performance because it plays a major role in the stall process. Transition can be accelerated by increasing the free-stream turbulence with wires or grids ahead of the airfoils, or by artificially boundary layer tripping near the airfoil leading edge. It appears from the literature review that, trip wires have a remarkable effect on the boundary layer transition due to the formation of the wake behind the trip wires, Refs. [12] to [14]. The effect of artificial transition on the aerodynamic performance and the wake development behind the airfoil trailing edge are not completely clarified.

In this paper, an experimental study was conducted to examine the effects of the boundary layer tripping and transition on the aerodynamic performance and a wake of a cambered airfoil. The NACA-2415 airfoil is used in this investigation. Wake-velocity profiles are measured at five values of angle of attack, namely θ = -10, -5, 0, 5 and 10 degrees, while trip wires having diameters of 0.3 and 0.8 percent of the airfoil chord (0.3 and 0.8 mm respectively) were separately imposed near the leading edge of the airfoil. The data for the tripped flows have been compared with each other and with that for the untripped airfoil flow.

2- EXPERIMENTAL APPARATUS AND PROCEDURE

2-1 Wind Tunnel

The experiments were carried out in a low turbulence open - type wind tunnel. The wind tunnel employed in these experiments consists of six parts centeraxial fan, wide angle diffuser, test section, contraction with 0.25 to 1.0 diameter ratio, settling chamber and the entrance portion. Honeycomb and graduated screens are installed in the settling chamber for breaking the free-stream turbulence which is less than 0.05 % at air velocity of 55 m/s. The control panel of the wind tunnel consists of a variable frequency controller and a remote control speed device. The air speed in the test section can be controlled from the control panel of the wind tunnel using a pre-calibrated curve. Calibration for the wind tunnel air speed against the frequency of the wind tunnel controller was made using a pitot-tube and a pressure transducer. The pressure was converted into speed and a straight line relation between the air speed and the frequency was obtained. The test section, which is made of prespex, has a square cross-section 305×305 mm and 610 mm long. At the top wall of the test section, a traversing unit was mounted and a small slot in the longitudinal direction was made to accommodate the probe holder. The airfoil

model is horizontally mounted by a vertical adjustable strut which allows the airfoil to be inclined at the desired angle of attack.

2-2 Airfoil model and instrumentation

Wind tunnel tests were conducted with a two-dimensional NACA-2415 airfoil, Fig. (1). The airfoil model was made of a filled epoxy resin. The chord (c) was 100 mm and the span was 300 mm. The tested airfoil model has a maximum thickness of 15 percent of the chord and the maximum camber equal to two percent of the airfoil chord which located at 40 percent of the chord, measured from the leading edge. Static pressure taps were drilled normal to the airfoil surfaces with 1mm diameter. The taps are distributed at the airfoil upper and lower surfaces. The tap locations on the upper and lower surfaces are presented in Fig. (1). The airfoil was tripped by separately placing two-different trip wires with diameter to airfoil chord of 0.003 and 0.008 near the leading edge, namely at 5 percent of the airfoil chord . The trip wires are designated as trip-1 and trip-2, respectively. The aerodynamic performance of the untripped and tripped airfoils were measured at angles of attack ranging from zero to 20 degrees. The measurements of the drag and lift were made via the force balance. Several investigators used this method at low Reynolds number and at low-to-moderate angles of attack, Ref. [15]. The lift and drag forces which give the airfoil performance were measured using the calibrated lift and drag dynamometer. The measurements of mean velocity profiles in the wake region were conducted at different locations downstream the tested airfoil, namely x/c = 0.5, 0.75, 1.0, 1.5 and 1.7 . A calibrated five-holes probe of 5 mm diameter was used to measure the wake-mean velocity profiles, at constant Reynolds number of 1.61×10^5 based on the free-stream velocity and the airfoil chord. The static pressure distributions along the upper and lower surfacses of the tripped and untripped airfoils were measured using multi-tube inclined water manometer. The measurements of pressure distribution, the lift and drag forces were carried out at different Reynolds number ranged from 3×10^4 to 1.92×10^5 . The NACA-2415 airfoil sections was initially tested without trip wires to obtain agreement with previous studies, Ref. [16]. Effects of boundary layer-tripping on the lift and drag coefficients as a function of angle of attack and Reynolds number were tested. In addition, the wake flow parameters downstream the airfoil with and without tripping were obtained.

The experimental errors in the measurements were calculated using Kline and McClintock technique [17]. It was found that, the error in the mean velocity measurements to be in the range of ± 1% at the maximum calibration velocity of 50 m/s. The corresponding error in the measured static pressure coefficient was about ± 1.2% . The uncertainty in the velocity defect was about 2.1% .

3- EXPERIMENTAL RESULTS AND DISCUSSION

3-1 Pressure Distribution

A representative sample of pressure coefficient data are shown in Fig. (2) for the angle of attack range of zero to 10 degrees and for Reynolds number of 1.61×10^5. For untripped airfoil, Fig. (2-a) indicates that the beginning of the adverse pressure gradient on the upper surface is very close to the leading edge. Also, the magnitude of the adverse pressure gradient increases significantly with increasing the angle of attack. On the lower surface these effects are just the opposite. As the angle of attack increases, the adverse pressure gradient decreases. However, the pressure coefficient on the lower surface for $\theta = 10$ degrees indicates a separated flow at $x/c = 0.2$ which is represent by a constant pressure coefficient. This separated region is followed by flow reattachment which is indicated by a negative pressure gradient. As a consequence, asymmetric separation patterns developed on the airfoil upper and lower surfaces. The adverse pressure gradient has a strong effect on boundary layer transition which controls the airfoil performance. The effect of placing a trip wire on the leading edge as an artificial roughness for accelerating the flow transition is shown in Figs. (2-b) and (2-c). For airfoil with trip-1, Fig. (2-b) shows the major part of the model upper and lower surfaces which is subjected to adverse pressure gradient for zero-angle of attack. Boundary layer transition points on the upper surface moves forward and rearward on the lower surface as the angle of attack increases. The peak value of the negative pressure increases with the increase of the trip-wire diameter, as shown for airfoil with trip-2 in Fig. (2-c). The effect of the angle of attack and trip-wire diameter on the maximum value of the negative pressure coefficient, which represents the transition point from laminar to turbulent flow, will be discussed in the following.

Figure (3) shows the airfoil peak value of the negative suction pressure coefficient, ($C_{P \, min}$), plotted against the angle of attack (θ), for the untripped and tripped airfoil and for two Reynolds numbers, namely Re = 0.831×10^5 and 1.61×10^5. It is seen from this figure that, the presence of trip wires increases the negative peak value of the pressure coefficient at zero-angle of attack. As the angle of attack (θ) increases, the adverse pressure gradient increases causing a large increase in the velocity at the leading edge and consequently a steep in the static pressure. It appears from Fig. (3-a) that, the stall angle of the untripped airfoil at Re = 0.831×10^5 reduces from 14 degrees to 12 degrees for the airfoil with trip-1. Thus, it is clear that the placement of the trip-1 actually degrades the airfoil performance, due to a leading edge stalling. The peak value of the negative pressure coefficient with trip-2 at Re = 0.831×10^5 is slightly higher than that with trip-1 before the airfoil experiences abrupt leading edge stall. The stall angle of the airfoil with trip-2 is increased again to the same stall angle in the case of untripped airfoil ($\theta = 14$ degrees), while the leading edge separation still forms in this case. When Reynolds number increases to 1.61×10^5, Fig. (3-b), the untripped airfoil experiences a trailing

edge stall at θ = 16 degrees as seen by the gradual decrease of C_{Pmin} immediately after stalling condition. With trip-1 in place, the airfoil develops consistently lower peak suction levels than that when it is untripped. Also, the stall angle of 14 degrees is lower than the stall angle of 16 degrees for the untripped case. The airfoil performance with trip-2 is worse than that of the untripped airfoil and tripped airfoil with trip-1. Also, the peak suction level reaches a maximum value at θ = 10 degrees and then falls gradually, indicating a trailing edge stalling airfoil. It appears from these figures that, this radical change in steady stall behavior demonstrates the sensitivity of the flow to the design of the tripping mechanism and points to the need for properly tripping the airfoil.

3-2 Aerodynamic Performance

A convenient parameter to measure the effectiveness of an airfoil is its lift-to-drag ratio (C_L / C_D). The maximum value of this quantity gives a good indication of the airfoil effectiveness. Figure (4) shows how the airfoil effectiveness vary with Reynolds number at a given angle of attack for untripped and tripped airfoils. Generally, it can be seen from this figure that, at lower values of Reynolds number where the viscous effects are relatively large, causing high drags and limiting the maximum lift-to-drag ratio, while at the higher values the lift-to-drag ratio improves. As discussed previously, increasing the angle of attack at small Reynolds number causes an abrupt leading edge stall and hence sudden severe deterioration in airfoil effectiveness, as shown in Fig. (4-a). For tripped airfoil, Figs. (4-b) and (4-c), the drag introduced by placement of any trip wire reduces the energy available to overcome the adverse pressure gradient, possibly resulting in separation at lower values of the pressure gradient. The effect of tripping on the drag coefficient at different Reynolds number is shown in Fig. (5). It appears that, a large part of the drag increment may be associated with airfoil tripping results from a forward movement of transition. The induced drag by the trip wires causes a more reduction in the airfoil effectiveness compared with that of the untripped airfoil. This occurs due to that, the wire diameter may be larger than the boundary layer thickness. For a given tripping at the leading edge, the lift-to-drag ratio increases slowly with increasing Reynolds number, especially after stalling conditions. This analysis demonstrates that when selecting a trip wire for the transition purpose must be produce turbulence and suppress a laminar separation without causing the turbulent boundary layer to become thick. A thick turbulent boundary layer may again suffer separation or at least cause an increase in drag.

3-3 Mean Velocity Distributions

The distributions of the experimental mean velocity behind the untripped cambered airfoil NACA-2415 for five different longitudinal locations is shown in Fig. (6). In Fig. (6-a), the angle of attack (θ) is taken to be −10, -5 and 0 degrees, while the mean velocity profiles are plotted in Fig. (6-b) at θ = 0, 5

and 10 degrees. It is not possible to carry out measurements before x/c = 0.5 due to the presence of violent eddies and flow separation in the trailing edge region. For negative angle of attack, as shown in Fig. (6-a), it appears that the mean velocity in the outer region of the wake is slightly increases as the angle of attack decreases from zero to −10 degrees. In this case, the flow is accelerated on both the upper and lower airfoil surfaces because the flow is subjected to a favourable pressure gradient. In addition, the minimum velocity in the wake region decreases with decreasing the angle of attack and the velocity distributions are symmetric with respect to the wake center. The minimum velocity increases with downstream locations. In other words, the velocity profiles in the presence of negative pressure gradients are characterized by a highly dissipative vortical core inside the wake region surrounded by external flow region. This results from the strong interaction between the wakes of the upper and lower sides because separation occurs close to the trailing edge. Overall, it may be considered that the effect of streamline curvature on the mean velocity defect distribution is small in case of negative attack angle or favorable pressure gradient. As the angle of attack increases from zero to 10 degrees, the separation of the developed boundary layer on the upper surface of the airfoil is due to an adverse pressure gradient. The separation occurs upstream of the trailing edge forming a re-circulation region, which has a high turbulence intensity, and a turbulent wake is formed. This is reflected on the mean velocity profiles behind the airfoil as shown in Fig. (6-b). It is observed from Fig. (6-b) that, the velocity distribution exhibits a strong asymmetric character with higher velocities at the upper region of the airfoil. This asymmetric behaviour is a result of the existing an adverse pressure gradient across the wake and the streamline curvature effects. The difference between the edge velocities of the wake indicates the magnitude of the net pressure variation across the wake. It is noticed from Fig. (6-b) that, the difference between the wake edge velocities is still found up to the last measured location, x/c = 1.7 . This occurs due to that, the boundary layer separation unsymmetrically from both upper and lower airfoil surfaces which causes momentum transfer from lower to upper surface. However, increasing the angle of attack results in a decrease in the wake velocity defect which is indicated with increasing of the minimum velocity.

Figure (7-a) reflects the effect of placing a trip wire with different diameters near to the leading edge on the wake velocity profiles downstream the airfoil, at zero-angle of attack. The velocity profiles shown in Figs. (7-b) and (7-c) are plotted for angles of attack of −10 and 10 degrees, respectively. The mean velocity profiles downstream of the untripped airfoil are included in these figures for comparison purpose. For θ = -10, it appears from Fig. (7-a) that, the boundary layer tripping did not affect strongly the wake velocity profiles downstream the airfoil. For airfoil with trip-2 and zero angle of attack, Fig. (7-a), the wake center is shifted towards the lower surface. For θ = 10 degrees, the presence of trip wires with adverse pressure gradient strongly affect the wake velocity profiles due to the presence of violent eddies and

asymmetric flow separation. The effect is quite evident for airfoil with trip-2, particularly in the near wake region from the trailing edge, x/c = 0.5 and 0.75 . In the near wake region, the velocity profiles show more vortex pairs within the wake compared with the untripped case. This may be occurred due to the formation of the wake behind the trip wire and the boundary layer separates asymmetrically from the two airfoil surfaces, as discussed previously. In this case, there is a weak interaction between the wakes of the upper and lower surfaces causing different minimum velocity peaks in the upper and lower regions of the wake. Further downstream at x/c = 1.0, the interaction between the wakes becomes strong indicating a minimum velocity at the wake center, due to the high momentum flow by the vortex pairs. Much further downstream, the velocity profile defect starts to decrease. The airfoil with trip-2 is characterized by larger velocity defect and the velocity profiles showed asymmetrical wake.

3-4 Wake Flow Parameters

Sreenivasan and Narasimha [18] and Townsend [19] have characterized a plane wake by two parameters (b) and (Δu), where b is the half-wake width and Δu is the wake defect velocity. The wake center is defined as the location of maximum velocity defect (Δu_m). The maximum velocity defect Δu_m normalized by the free-stream velocity (U_0) and the half-wake width (b) normalized by the airfoil chord (c). A schematic representation of the wake parameters for symmetrical and asymmetrical cases are shown in Fig. (8). The parameters which represent the general behaviour of the wake downstream the untripped cambered airfoil (NACA-2415) are selected and shown in Fig. (9) for angles of attack of –10, 0, and 10 degrees. It is observed from this figure that the wake half-width (b) is not same on the two sides of the wake. For θ = -10 and zero degrees, the half-width of the wake is more on the lower side of the cambered airfoil than that on the upper side. The variation of an average of the values of the half-widths on the upper and lower sides ($\bar{b}$) are included in the figure. As shown in Figs. (9-a) and (9-b), the average wake width increases with increasing x/c, because of the diffusional processes that take place in the free turbulent shear flow. For θ = 10 degrees, Fig. (9-c), the half-width of the wake on the upper side of the wake is more than that on the lower side due to the presence of adverse pressure gradient which causes separation flow on the upper and lower surfaces of the airfoil. It is seen that, the width of the wake was found to be strongly dependent upon the angle of attack. Therefore, it can be concluded that, the pressure gradient and separation location on the airfoil significantly control the growth of the half-width of the wake and this, in turn, controls the wake size downstream the airfoil. The growth of the average half-wake width is faster for a positive angle of attack than that of zero and negative angle of attack. The variation of the maximum value of the dimensionless mean velocity defect ($\Delta u_m / U_0$) with x/c for different attack angles are included in the figures. As pointed out, $\Delta u_m / U_0$ decreases as x/c increases, for θ = -10 and zero angle of attack. The wake

122

velocity defect decrease resulting in a continuous increase of the wake width with downstream location. The decay rate of dimensionless maximum velocity defect in the presence of positive pressure gradient ($\theta = 10$ degrees) is slower than that in the case of zero and negative pressure gradients. This occurs due to the presence of asymmetric separation patterns which are formed on the upper and lower airfoil surfaces, as discussed previously in section (3-1).

The wake parameters downstream the tripped airfoil are shown in Fig. (10) for different trip-wire diameters and different attack angles. The experimental results indicate that, the average wake width strongly affected with the size of the trip-wire. For $\theta = -10$ degrees, the average wake width with the untripped airfoil is more than that of the tripped airfoil. On the other hand, the presence of tripping slightly increases the rate of decay of the maximum velocity defect and reducing its value in the location immediately downstream the airfoil. Increasing the angle of attack from -10 to 0 and 10 degrees delays the decay of the maximum velocity defect. This occurs because the separation location on the upper surface of the airfoil moves forward and rearward on the lower surface in the presence of tripping wires. Therefore, it can be concluded that, the presence of tripping slightly influences the decay of the maximum mean velocity defect in the case of zero and negative angles of attack. For $\theta = 10$ degrees, the maximum velocity defect increases with increasing the trip-wire diameter (trip-2) and hence the rate of decay is decreased.

3-5 Wake Similarity

Figures (11) to (13) show the lateral distribution of the non-dimensional mean velocity defect for different longitudinal locations and for various values of angle of attack. The normalized mean velocity defect are plotted for the tripped and untripped airfoil. The mean velocity defect is normalized by its maximum value (Δu_m) and the lateral distance by the average wake width ($\bar{b}$). The purpose for normalizing the mean velocity defect and the lateral distance is to check the existence of similarity for mean velocity defect profiles. In these figures, the experimental results (symbols) are compared with the developed theory for straight wakes (solid and broken lines) Ref. [20] and [21]. The solid and broken lines are based respectively on, $\Delta u / \Delta u_m = e^{-\phi^2}$

and $\Delta u / \Delta u_m = \left(1 - 0.293 \, \phi^{1.5}\right)^2$ where $\phi = (y - y_c)/\bar{b}$ and y_c is the lateral distance measured from the wake center. It appears from Fig. (11) that, the results of mean velocity defect in the case of $\theta = -10$ degrees, which leads to a favourable pressure gradient, confirm the existence of similarity and almost identical to the straight wake. It is observed also from Fig. (11) that, the wakes are wider on the lower side of the wake. Hence, it may be considered that the effect of airfoil curvature and the favourable pressure gradient on the mean velocity defect profiles are small. This is observed for tripped and untripped airfoil. Increasing the angle of attack from -10 to zero and 10 degrees increases the degree of asymmetry in the mean velocity defect profiles, as shown in Figs. (12) and (13). This asymmetric behaviour is a result of the

123

existence lateral pressure gradient associated with wake curvature. In case of boundary layer tripping, the individual velocity defect profiles are characterized by a highly dissipative vortical core inside the wake region surrounded by an external potential flow region. In addition, the presence of trip wires causes two peak values of the mean velocity defect in the wake region. This may be attributed to leading edge separation and due to the wake of the trip wires located near to the leading edge of the airfoil, Refs. [12] and [13]. Figures (11) to (13) show that the similarity profiles of tripped and untripped airfoil are well described with the previous developed theory for the case of the negative angles of attack. For zero and positive angles of attack, asymmetry about the wake center in the similarity profiles is reduced when compared to the asymmetry in the mean velocity profiles due to the appropriate normalization. However, the comparison between the experimental results and the developed theory given in Refs. [20] and [21] indicates that the similarity profiles are not represented by this theory.

4- CONCLUSIONS

On the basis of an experimental investigation on the effects of the boundary layer-tripping on the performance and the development of an airfoil wake, the following conclusions can be drawn,

1- The results showed that the airfoil performance is sensitive to the tripping mechanism. The stall flow was extremely affected with the trip used and hence to the turbulence level in the flow immediately downstream the trip.

2- The drag coefficient for the airfoil with trip-wires becomes higher than that the corresponding value for the untripped airfoil. This causes a more reduction in the airfoil effectiveness.

3- The mean velocity distribution behind the untripped airfoil exhibited asymmetric character in the case of positive angles of attack due to the existing of an adverse pressure gradient across the wake and curvature effects.

4- For untripped airfoil, the wake centerline velocity (minimum velocity) recovers faster in the case of negative angles of attack than that in the case of zero and positive angles of attack. The wake width is not the same on both sides of the wake.

5- The wake velocity profiles are observed to be asymmetrical when the wake is influenced by the positive pressure gradient and boundary layer-tripping. The boundary layer-tripping did not affect strongly the wake velocity profiles in case of negative angles of attack. Increasing the angle of attack causes a strong distortion in the wake velocity profiles due to the presence of violent eddies and asymmetric flow separation.

6- The presence of tripping slightly influences the decay of the maximum mean velocity defect in the case of zero and negative angles of attack. For $\theta = 10$ degrees, the maximum velocity defect increases with increasing the trip-wire diameter (trip-2) and hence the rate of decay is decreased.

7- For negative angle of attack and untripped airfoil, the similarity in the mean velocity profiles for the pressure or suction side is almost identical to the straight wake profile. Asymmetry in the velocity profiles behind the tripped and untripped airfoils increases with increasing the angle of attack and the trip wire diameter.

NOMENCLATURE

b   half-wake width

$\bar{b}$ average half-wake width, $0.5(\,b_u + b_\ell\,)$

c   airfoil chord

C_D drag coefficient, $D/(\,0.5\,\rho\,U_o^2\,c\,)$

C_L lift coefficient, $L/(\,0.5\,\rho\,U_o^2\,c\,)$

C_P static-pressure coefficient, $(\,P - P_o\,)/(\,0.5\,\rho\,U_o^2\,)$

D   drag force

L   lift force

P   static pressure

P_o reference static pressure

Re   Reynolds number, $U_o\,c\,/\,\nu$

U_o free-stream velocity

u   fluid-velocity at a distance y

u_c minimum velocity at the wake centerline

Δu wake velocity defect

x   streamwise-direction with origin at the leading edge

y   crosswise-direction

θ angle of attack

ρ fluid density

ν kinematic viscosity

Subscripts

c   wake centerline condition

ℓ lower side of the wake

m   maximum conditions

min   minimum conditions

o   free-stream value

u   upper side of the wake

REFERENCES

1- So, R. M. C. and Mellor, G. L., " Experiment on Convex Curvature Effects in Turbulent Boundary Layers", J. Fluid Mechanics, Vol. 60, 1973, pp. 43-62

2- So, R. M. C. and Mellor, G. L., "Experiment on Turbulent Boundary Layer on A Concave Wall", Aernautical Quarterly, Vol. XXVI, 1975, pp. 35-40

3- Ramaprian, B. R. and Shiraprasad, B. G., " Mean Flow Measurements in Turbulent Boundary Layers Along Mildly Curved Surfaces", AIAA J. Vol. 15, No. 2, 1977, pp. 189-196.

4- Bradshaw, P., "The Analogy Between Streamline Curvature and Buoyancy in Turbulent Shear Flow", J. Fluid Mechanics, Vol. 36, 1969, pp. 177-191.

5- Castro, I. P., and Bradshaw, P., " The Influence of A Highly Curved Mixing Layer", J. Fluid Mechanics, Vol. 73, 1976, pp. 265-304.

6- Pal, S., " Free-Stream Turbulence Effects on Wake Properties of A Flat Plate at An Incidence", AIAA J., Vol. 23, No. 12, 1985, pp. 1868-1871.

7- Merz, R. A., " Turbulence Intensities in The Near-Wake of A Semi-Elliptical After body," AIAA J., Vol. 24, No. 12, 1986, pp. 2038-2040.

8- Pal, S. and Raj, R., " Wake Behavior in The Presence of Free-Stream Turbulence", J. Engineering for Power, Vol. 103, 1981, pp. 490-498.

9- Nakayama, A., "Curvature and Pressure Gradient Effects on A Small-Defect Wake", J. Fluid Mechanics, Vol. 175, 1987, pp. 215-246.

10- Diaz, F., Gavalda, J., Kawall, J. G., Keffer, J. F., and Giralt, F., "Asymmetrical Wake Generated by A Spinning Cylinder", AIAA J., Vol. 23, No. 1, 1985, pp. 49-54.

11- Lissaman, P. B. S., " Low Reynolds Number Airfoils", Annual Review of Fluid Mechanics, Vol. 15, 1983, pp. 223-239.

12- Gibbings, J. C., Goksel, O. T., and Hall, D. J., " The Influence of Roughness Trips Upon Boundary-Layer Transition", Part 1. Characteristics of Trip Wires", Aeronautical J. , Oct. 1986, pp. 289-301.

13- Gibbings, J. C., Goksel, O. T. and Hall, D. J., " The Influence of Roughness Trips Upon Boundary-Layer Transition", Part 2. Characteristics of Single Spherical Trips", Aeronautical J., Nov. 1986, pp. 357-367.

14- Chandrasekhara, M. S., Wilder, M. C., and Carr, L. W., " Boundary-Layer-Tripping Studies of Compressible Dynamic Stall Flow", AIAA J., Vol. 34, No. 1, 1996, pp. 96-103.

15- Abtahi, A. A. and Marchman, J. F., " Aerodynamics of An Aspect Ratio 8 Wing at Low Reynolds Numbers", J. Aircraft, Vol. 22, July 1985, pp. 628-634.

16- Abbott, I. H. and Von Doenhoff, A.E., " Theory of wing sections ", Dover publications, INC., New York, 1949.

17. Kline, S. J. and McClintock, F. A. " Describing The Uncertainties in Single-Sample Experiments ", ASME, Mechanical Engineering Journal, Jan. 1953, pp. 3-8.

18- Sreenivasan, K. R., and Narasimha, R., "Equilibrium Parameters for Two-Dimensional Turbulent Wakes", J. Fluids Engineering, 104, 1982, pp. 167-170.

19- Townsend, A. A., " The Structure of Turbulent Shear Flows", Cambridge University Press, Cambridge, England, 1976.

20- John, J. and Schobeiri, M. T., " Development of A Two-Dimensional Turbulent Wake in A Curved Channel with A Positive Streamwise Pressure Gradient", ASME, J. Fluids Engineering, Vol. 118, 1996, pp. 292-299.

21- Schlichting, H., " Boundary layer theory", 6th ed. 1968, McGraw-Hill, New York.
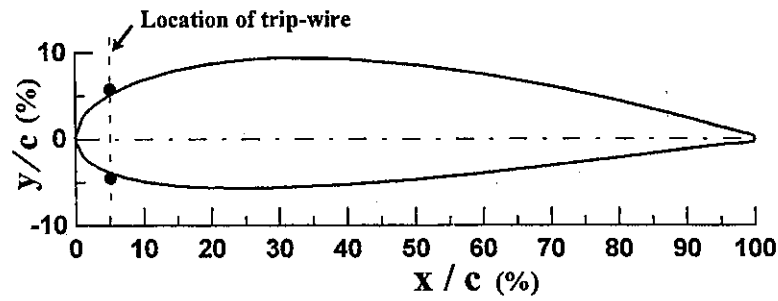
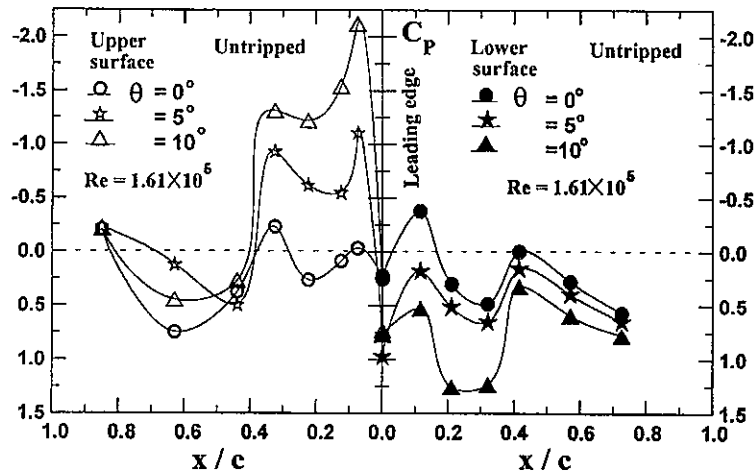**Tap-locations on the upper surface**

Tap No.	1	2	3	4	5	6	7	8
x / c (%)	0	7.5	12.5	22.5	32.5	44	63	85

Tap-locations on the lower surface

Tap No.	1	2	3	4	5	6	7
x / c (%)	0	11.5	21	32	41.5	57	72.5

Fig. (1) Model profile of NACA-2415 airfoil

(a)

(b)

Figure (2-a) and (2-b)

127
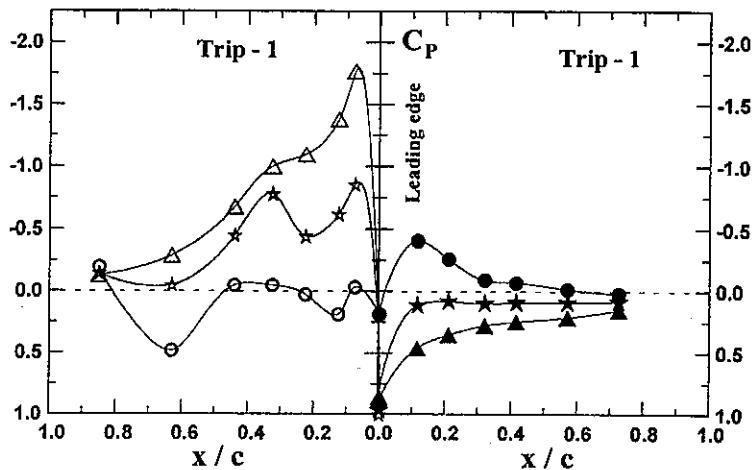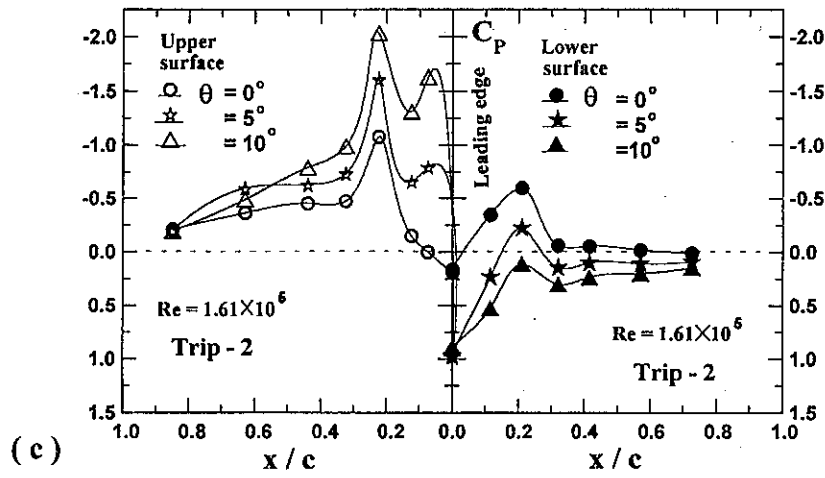
Fig. (2) Effect of angle of attack on the pressure coefficient of untripped and tripped airfoil
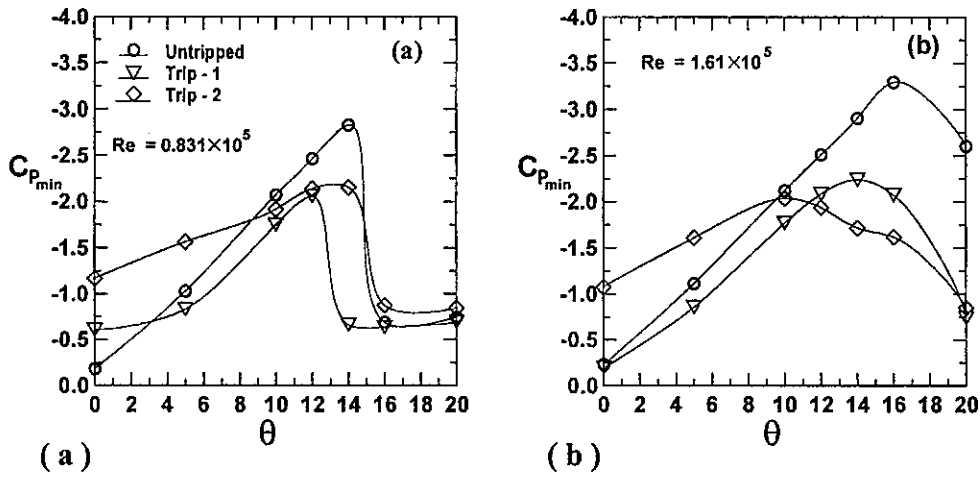
Fig. (3) Effect of tripping on the minimum pressure coefficient
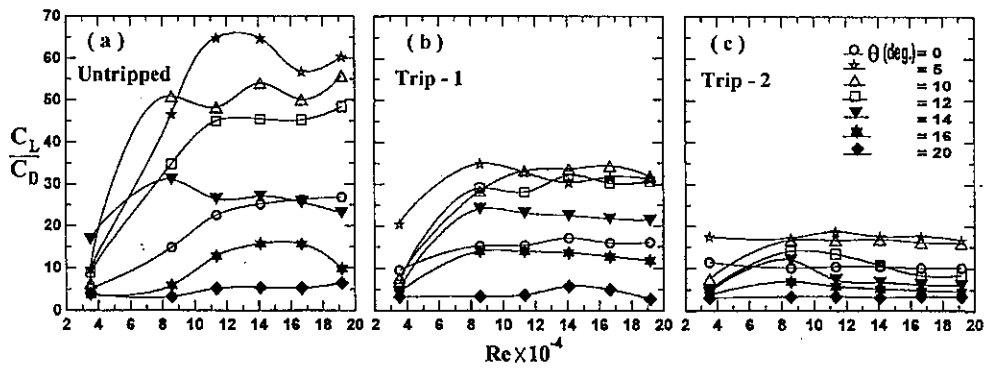
Fig. (4) Effect of angle of attack on the effectiveness of untripped and tripped airfoil

128
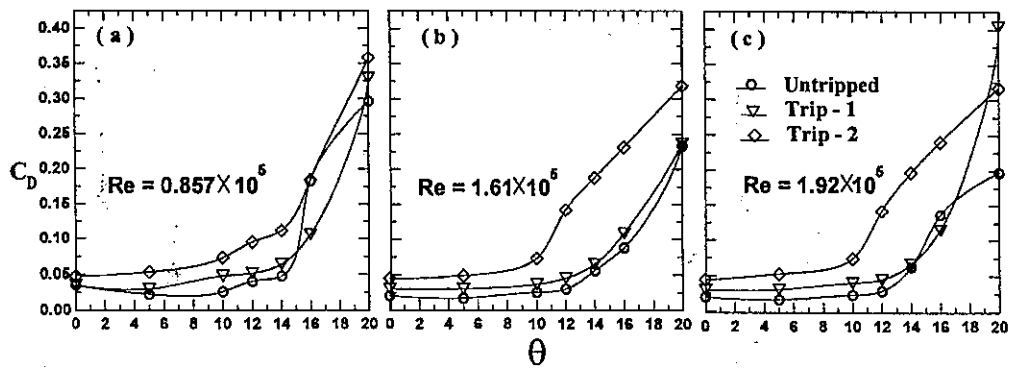
Fig. (5) Effect of tripping on the drag coefficient

(a)

(b)
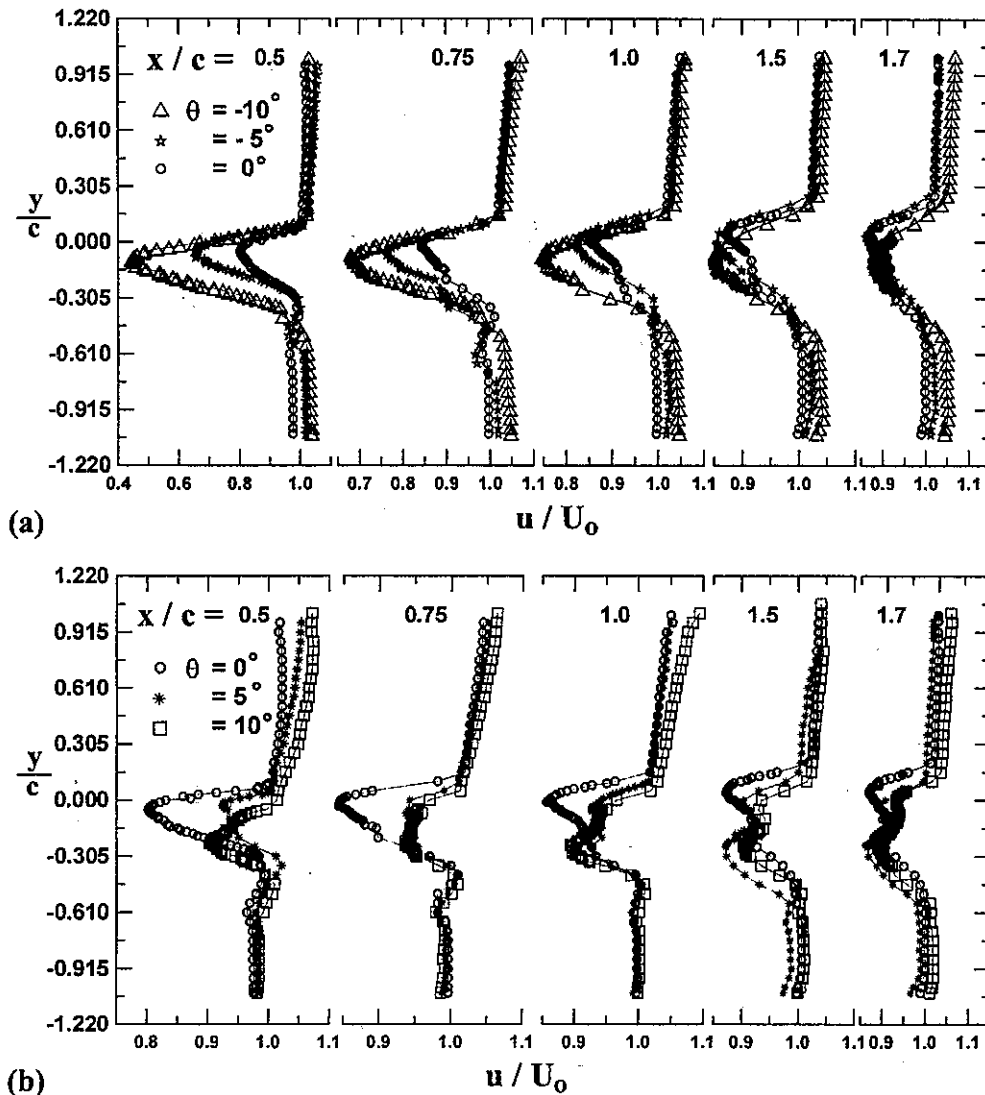
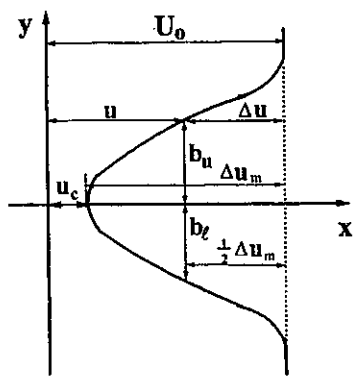**Fig. (6)** Effect of angle of attack on mean longitudinal velocity distributions for untripped airfoil, Re = 1.61×10^5 .

129
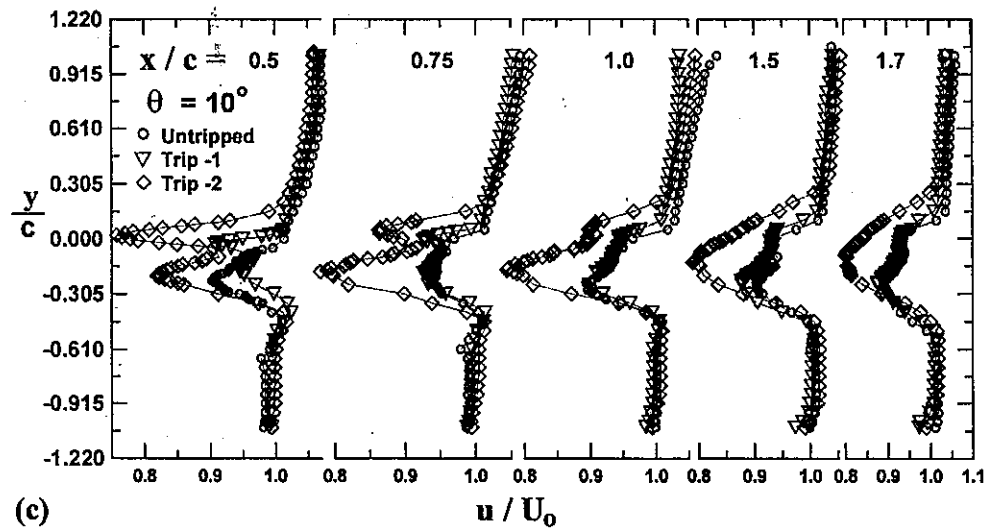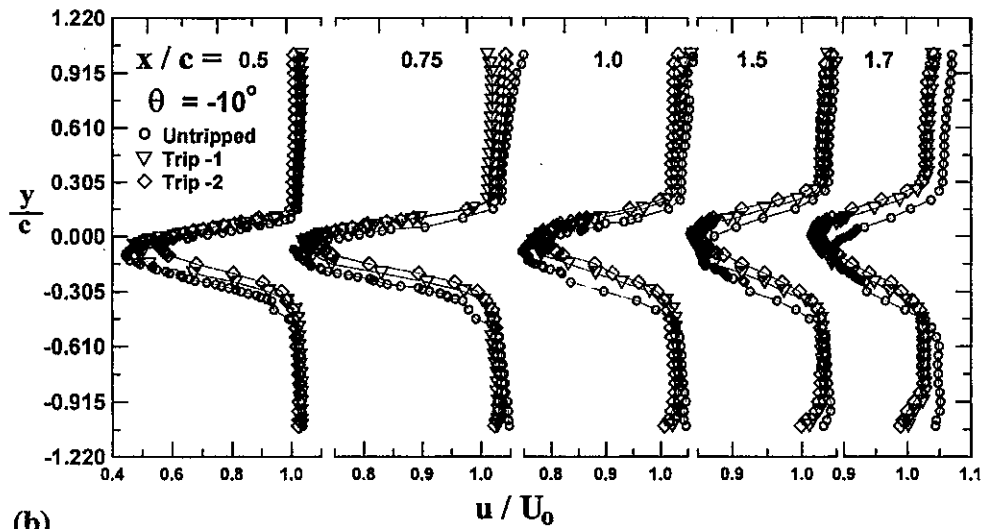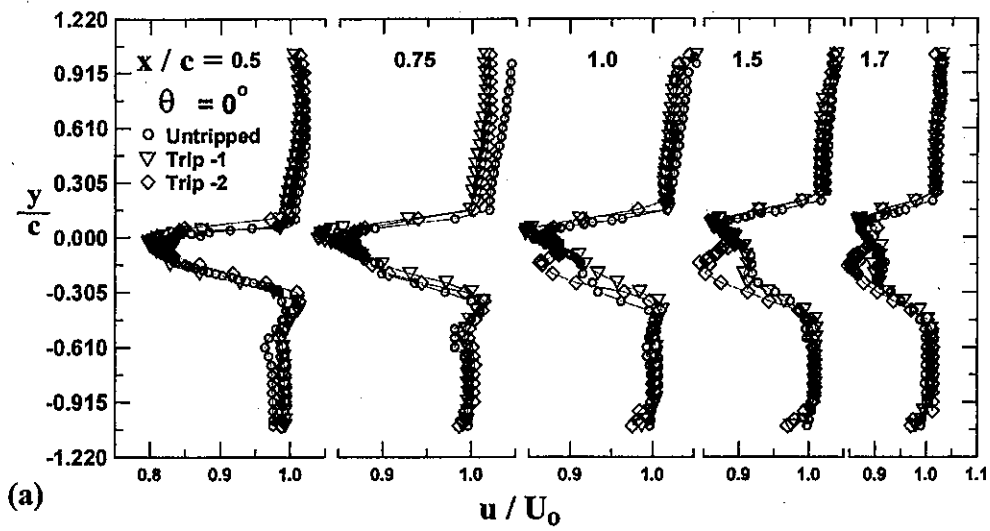
Fig. (7) Effect of tripping on the longitudinal velocity distributions, Re $= 1.61 \times 10^5$.
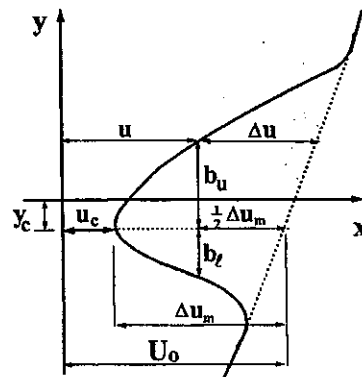
Symmetric wake   Asymmetric wake
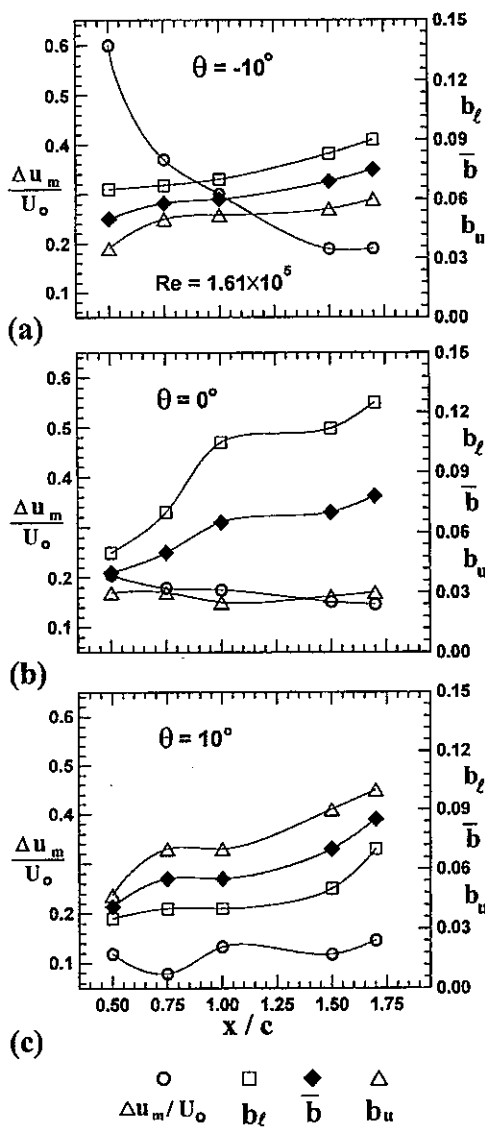
Fig. (8) Definition sketch of wake parameters

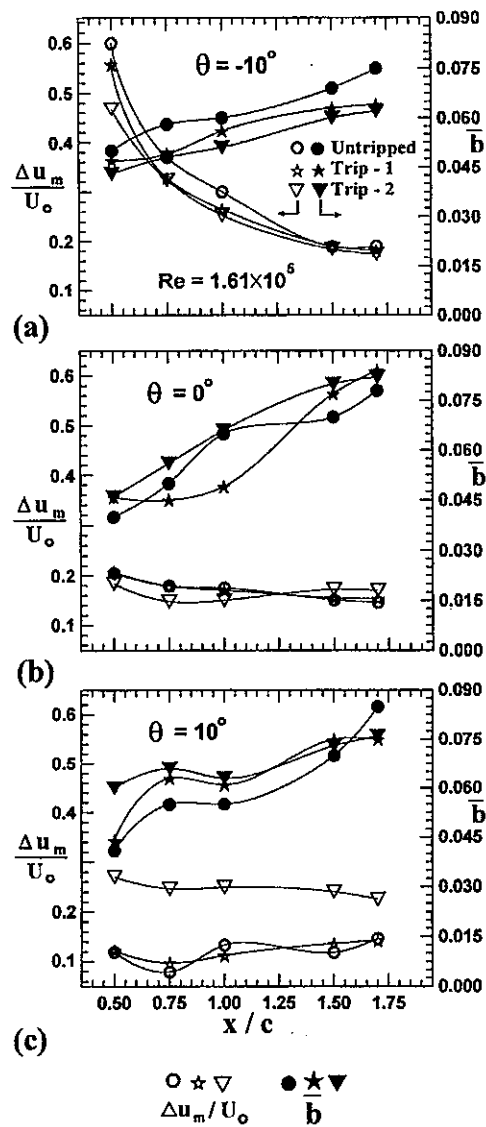**Fig. (9)** Wake flow parameters
for untripped airfoil

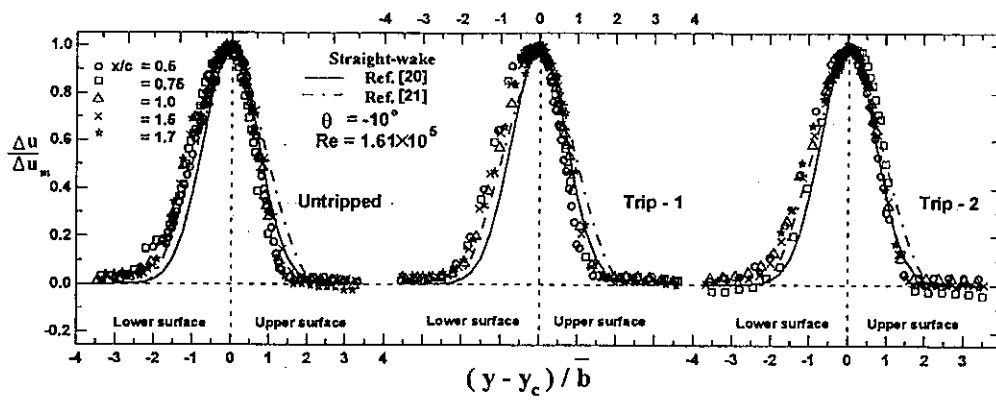**Fig. (10)** Effect of tripping on wake
flow parameters

131

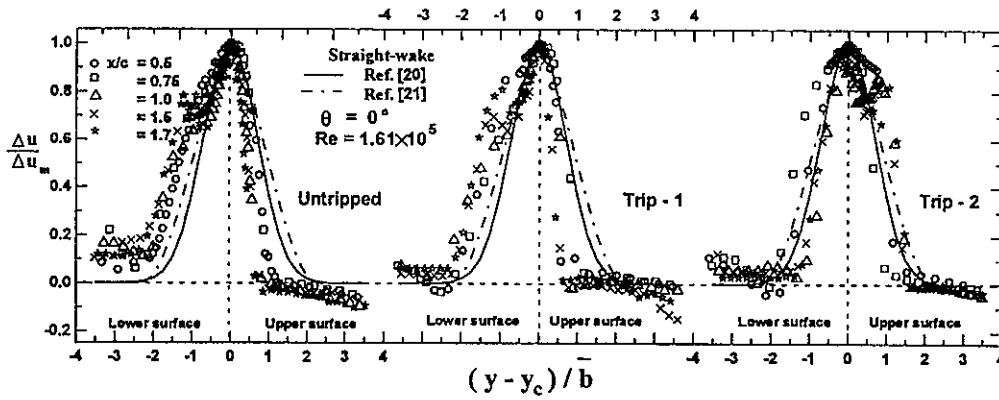**Fig. (11)** Normalized velocity defect for $\theta = -10$ degrees

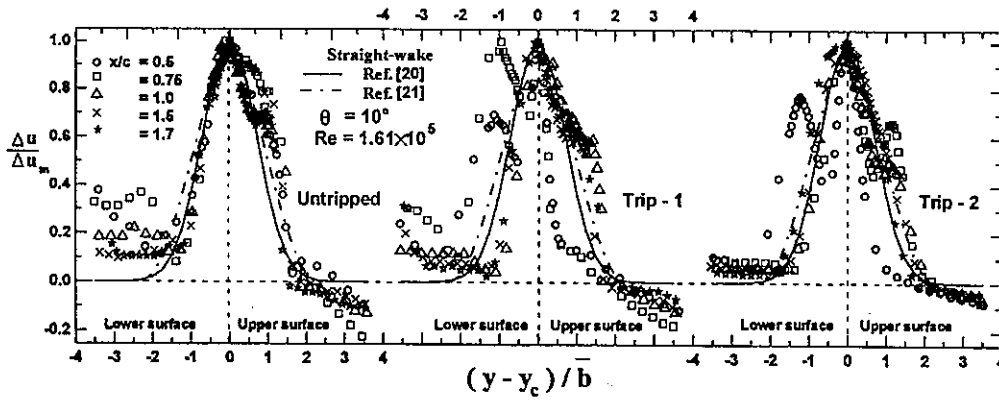**Fig. (12)** Normalized velocity defect for zero angle of attack

Fig. (13) Normalized velocity defect for $\theta = 10$ degrees

132

عنوان البحث :

(دراسة تعثر الطبقة المتاخمة على خصائص المخر خلف سطح انسياب هوائى مقوس)

د. حسن عوض عبد الله

قسم هندسة القوى الميكانيكية ـ كلية الهندسة بشبين الكوم ـ جامعة المنوفية

ملخص البحث :

يوضــح هذا البحث دراســة معمليــة لدراســة تـأثير تعثر الطبقــة المتاخمــة علـى الخصائص الأيروديناميكية لسطح إنسياب هوائى مقوس (NACA-2415)، وكذلك تأثير ذلك التعثر على مخر السريان الـذى يتكـون خلـف هذا السطح. هذه الدراسة لـها تطبيقات كثيرة منها السريان على ريش التربينات والضواغط وكذلك علـى أجنحـة الطائرات. تم إستخدام سلك العثرة (trip-wire) بالقرب من حافة المقدمـة للأيروفيل لتوليد تعثر الطبقة المتاخمة الذى يساعد على عملية الإنتقـال مـن السريان الرقائقى إلـى السريان الإضطرابى بسرعة. أجريت الدراسة المعملية على سطح إنسياب هوائى بـدون تعثر للطبقة المتاخمة ، وأيضا فى وجود تعثر بإستخدام أسلاك بأقطار مختلفة.

تـم إجراء قياسات لتوزيع الضغط الإستاتيكى علـى السـطح العلـوى والسـفلى للأيروفيل ، وكذلك تم إجراء قياسات لمعاملى الرفع والمقاومة. كذلك أجريت القياسات المعملية عند أرقـام رينولـدز وزوايا هجـوم مختلفة. ولدراسة التأثير علـى مخر السريان خلف سطح الإنسياب الـهوائى ، تـم قيـاس توزيع السرعة فى منطقـة المخر القريبة من السطح. تم قياس عرض المخر ونموه فى حالة وجود التعثر وفى حالـة عـدم وجوده ودراسة تأثيره على أداء هذا السطح.

أظهرت النتائج المعملية أن أداء الأيروفيل يتـأثر بقـوة بطريقـة تعـثر الطبقـة المتاخمة، حيث يتأثر أقصى أداء للأيروفيل بقطر سلك التعثر. يقل أداء الأيروفيل بزيـادة قطر سلك التعثر نظرا لزيادة معامل المقاومة. كذلك بينت النتائج أن توزيـع السـرعة متماثل فى منطقة المخر خلف الأيروفيل فى حالة زوايـا الهجوم السالبة وفى حالـة وجود وعدم وجود التعثر. بينما أوضحت النتائج تشوه وعدم تماثل توزيع السرعة فى منطقـة المخر عند زوايا الهجوم الموجبة ، وتزيد درجـة التشوه لتوزيع السرعة بزيـادة زاويـة الهجوم وقطر سلك العثرة ، نظرا لتأثير تقوس خط الإنسياب ووجود تدرج موجب للضغط. تم مقارنة النتائج المعملية لـهذا البحث مـع العلاقات النظريـة المتاحـة للمخر المتماثل. أظهرت المقارنة تطابقا للنتائج المعملية مع العلاقات النظرية فى منطقة المخـر المتولد عندما تكون زوايا الهجوم سالبة.